Si epitaxial growth on Br-Si(100): How steric repulsive interactions influence overlayer development

G. J. Xu and J. H. Weaver
Department of Materials Science and Engineering, and Frederick Seitz Materials Research Laboratory, University of Illinois at Urbana-Champaign, Urbana, Illinois 61801, USA
(Received 17 May 2004; published 28 October 2004)

Scanning tunneling microscopy results show the consequences of Si adatom deposition onto Br-saturated Si(100)-(2×1). Those adatoms undergo an exchange reaction with Br and they are immobile at room temperature. In the low coverage regime, annealing to 650 K leads to dimerization, limited ordering, and the formation of short Si chains. Adatom capture by those chains produces features of even and odd numbers of atoms. Annealing at 700 K eliminates the odd chains, but diffusion is highly constrained by Br site blocking. With subsequent Si depositions, there is further nucleation of chains and chain growth. The local patterning of the Si chains reveals the influence of the Br steric repulsive interactions as out-of-phase structures were favored over in-phase structures around any given chain. Eventually, (3×2) adlayer patches develop. Second layer chains appear after the deposition of $\sim$0.3 ML, with layer-2 nucleation at antiphase domain boundaries. Bromine loss was observed, even at 650 K, and it is probably tied to the weaker bonding to single isolated Si adatoms.

DOI: 10.1103/PhysRevB.70.165321 PACS number(s): 68.43.Jk, 68.37.Ef, 81.10.Bk, 81.16.Rf

I. INTRODUCTION

Several recent studies have focused on the roughening and etching of Si(100) induced by halogen adatoms. Those studies have implicated the steric repulsive interactions among the halogens for a lowering of the desorption barriers for Si dihalides. Even more significantly, they have shown that those adsorbate interactions destabilize the (2×1) structure and lead to patches of (3×2) structure in which Si dimer rows alternate with atom vacancy lines to increase the separation between adatoms. The latter was a surprise because the Si surface was thought to be stable against such roughening.[1–7]

In this paper, we use atomic resolution scanning tunneling microscopy (STM) results to compare Si surfaces that are roughened by Br to those that evolve when Si adatoms are deposited onto a Br-saturated Si(100)-(2×1) surface. Our focus is on the adsorption and diffusion of Si adatoms and the nucleation and growth of the adlayer in the presence of Br. We show that the adatoms spontaneously undergo an exchange reaction, but that the presence of the strongly bound Br atoms prevents subsequent diffusion at room temperature. Site blockage by the Br is so effective and Si diffusion is so slow, even at 650–700 K, that it is possible to follow the onset of ordering and the growth of Si dimer chains. We show that the strong repulsive interactions of Br dictate the patterning of the adlayer as it is built up by continued deposition, and (3×2) patches dominate when the Br concentration is high. As subsequent layers start to form, they tend to have lower Br concentrations, and this alters the structures that appear.

Though the effects of halogen adsorbates on Si(100)-(2×1) have been studied extensively, these results offer further insights into the role of Br with regard to the Si regrowth structures and homoepitaxy. They also make possible comparisons with the H–Si(100) system where both experimental and theoretical studies have focused on Si and Ge overlayer growth and the role of H as a surfactant.

II. EXPERIMENTAL CONSIDERATIONS

The experiments were carried out in an ultrahigh vacuum system with an Omicron variable temperature STM and sample cleaning, Br deposition, and Si deposition capabilities (operating pressure $<5\times10^{-11}$ Torr). The Si wafers were *p*-type, B doped to 0.01–0.012 Ω cm, and oriented within 0.5° of (100) with miscut along [110]. Clean surfaces were prepared by degassing at 875 K for 12 h and then heating to 1475 K for 90 s at $<1\times10^{-10}$ Torr. The surface defect area was $\sim$0.01–0.02 ML, primarily in the form of dimer vacancies and C-type defects.

A solid state electrochemical cell was used as a source of Br_2. It was made from a mixture of AgBr with 5% $CdBr_2$. Clean Si surfaces were exposed to the source at room temperature to achieve full saturation. Si adatoms were provided by a commercial source that relied on Joule heating. The deposition rate was 0.006 ML s^{-1}, and the sample was kept at room temperature during deposition. Subsequent annealing cycles at 600, 650, or 700 K for 10 min allowed limited Si diffusion, and further Si deposition cycles made it possible to follow overlayer development as it was built up. The surface morphology was characterized with STM at room temperature after each deposition and annealing cycle. An optical pyrometer was used to monitor the sample temperature (reproducibility ±10 K). Both filled- and empty-state images were acquired with Pt/Ir tips in the constant current mode.

III. RESULTS AND DISCUSSION

A. Si–Br exchange on Br-terminated Si(100)

The deposition of Si on Br-saturated Si(100) results in Si exchange with Br but Si does not simply change places with

Br. Instead, it establishes a more complex bonding configuration. We speculate that Si can explore the 1×1 surface unit cell prior to bond formation, depending on dynamics associated with shedding the kinetic and condensation energies and the position on the potential energy surface where impact occurred. Subsequent motion is kinetically constrained at room temperature, and STM images obtained following 0.025 ML deposition revealed poorly ordered Si. From experiment, we see that isolated Si adatoms represent ~90% of the total features with dimers accounting for ~9%. These adatoms and adatom pairs are not mobile. In contrast, neither individual adatoms nor pairs are observed for Si deposition on clean Si at 300 K because the Si diffusivity is high and dimer chains form.[8,9]

Monte Carlo simulations were carried out to confirm that Si adatoms were not mobile on the Br–Si(100) surface in a physisorbed state prior to exchange. We found that the single adatom population was ~90% for 0.025 ML coverage if Si movement was forbidden and ~81% if one jump of 3.84 Å was allowed. The simulations also show that the probability of finding two adatoms on adjacent sites is ~9%. Thus, the results of no-diffusion match well with the experiment.

Site exchange analogous to that seen here has been reported in studies of Si and Ge growth on H–Si(00), with differences that would be related to the bond strength and size of the Br ion.[10–15] First-principles total-energy calculations of Si on H-terminated Si(100) indicated that Si–H exchange occurred without an activation barrier since the total energy decreased monotonically as a H atom was transferred from a substrate Si atom to a Si adatom and the Si adatom was bound to the substrate.[11,12]

B. Si ordering on Br–Si(100)-(2×1)

Figure 1 reproduces a high resolution image that makes it possible to identify the structures that form when the kinetic constraints of Sec. III A are eased somewhat. This empty-state image was acquired after a clean surface was saturated with Br, exposed to 0.06 ML of Si at room temperature, and annealed at 650 K for 10 min. The dimer rows run from bottom left to upper right with gray scale ovals that are composed of two Si atoms from adjacent rows. (In empty-state imaging, the middle of a dimer appears as a deep minimum.) Br is bound to each Si dangling bond on the terrace, and it quenches the dynamic buckling motion characteristic of dimers of the clean surface. Individual Br atoms can be resolved if the contrast is adjusted to emphasize them rather than the bright features. The bright features are one atomic layer higher than the substrate, and they are produced by Si–Br exchange. They are small and their density is high.

In ordered areas, it is possible to identify Br bound to the dangling bonds of the addimers. Direct counting reveals that about 1/3 of the sites on the addimer chains are bare, while the Br atoms are almost conserved on the terrace. (The determination of halogen coverages has been discussed by Xu *et al.*[6]) For example, the four Si atoms in the lower right circle are all terminated with Br, while the six in the dashed ellipse are Br free. The structure near the center is made up of four dimers, and the contrast indicates that all of the Si adatoms are terminated with Br, except the two marked with arrows. This can also be seen in the three-dimensional image of Fig. 1(b) where the two Br-free Si adatoms are lower than the other six. The distribution of bare sites indicates that bonding on terraces is stronger than on the addimer chains, an effect that is important when the Br concentration decreases and the chain area increases.

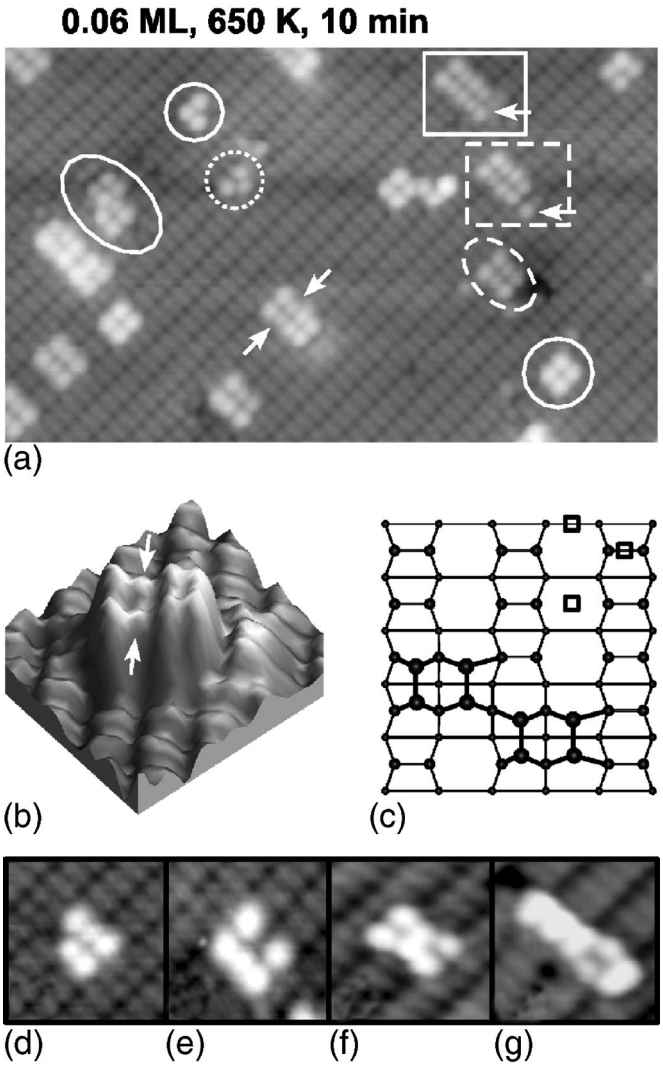

FIG. 1. (a) High resolution empty-state STM image (200×120 Å^2) showing Si overlayer features on Br-saturated Si(100). The Si adatom concentration is 0.06 ML and the surface had been annealed at 650 K for 10 min. Chains formed with both even and odd numbers of atoms. The Br concentration on the terrace was largely conserved, but some of the addimers were Br free; (b) three-dimensional image of a Si chain of eight atoms where the two adatoms marked with arrows are lower in profile, indicating that they are Br free [same chain visible in center of (a)]; (c) schematic of the positions of the three Si atoms inside the dashed circle that are marked with three squares, and antiphase connection of two segments inside the ellipse in (a); (d)–(g) show incomplete adatom chains; (d) and (e) are empty-state images (+1.7 V, 1 nA), while (f) and (g) are filled-state images (−1.7 V, 300 pA).

The solid and dashed circles at the upper part in Fig. 1(a) each contain three Si atoms. The positions of those in the dashed circle can be deduced from their distances to the substrate dimers. They are depicted as squares on the upper-right-hand side of Fig. 1(c), and their separation indicates that no covalent bonds have formed. Clusters of three features like this are common, suggesting a Br-mediated attraction that favors their formation.[16,17] The three atoms inside the solid circle show order since the upper two have dimerized and the bottom one is waiting for a partner. The addition of another atom would produce a tetramer like that in the circle at bottom right, the structure of which can be deduced from Fig. 1(c). The dashed rectangle of Fig. 1(a) draws attention to a chain of eight atoms and a separate Si adatom located on the next dimer row, identified by the arrow. This Si adatom can attach if it hops $a_0 = 3.84$ Å from the middle of the next dimer row to the trough, as in the solid rectangle.

Figures 1(d)–1(g) show adatom chains in various configurations. Figures 1(d) and 1(e) are empty-state images where there is a deep minimum between the atoms within a dimer and Figs. 1(f) and 1(g) are filled-state images where the minimum is offset by half a dimer unit. Figure 1(d) shows a single adatom attached to a two-dimer chain. This structure can convert to either a two- or three-dimer unit by losing or capturing a Si atom. Figure 1(e) shows a chain of five atoms, where one of the atoms in the middle is missing. Figure 1(f) shows a six atom chain where the middle atoms have dimerized and appear as ovals in the filled-state image. The two atoms at either end are distinct and, while they are attached to the chain, they do not appear to have dimerized. Equivalent chains with undimerized end atoms have been observed in studies of Br–Si(100) etching.[18] Apparently, Si atoms are trapped in potential minima that are induced by Br adsorbates. Si chains can grow or decay by capturing or losing individual Si atoms, and this structure probably represents an intermediate state. In the chain in Fig. 1(g), the atoms are dimerized except for the pair on lower right.

Chains can grow by end-to-end connection of segments that are either in-phase or out-of-phase. The solid ellipse in Fig. 1(a) identifies an out-of-phase connection where the two segments were offset laterally by one atomic unit, depicted in Fig. 1(c) without the Br atoms. A third growth mode involves the nucleation of a second row to establish features wider than one row. These islands have (2×1) symmetry and are favored for the clean surface. In the presence of a high concentration of Br, however, (2×1) islands are not favored because Br atoms on them are too close to one another (the steric repulsive interactions discussed below). Instead, chains tend to be separated by a line of single-atom vacancies, defining a (3×2) periodicity. This will have important implications as the Si coverage increases.

The filled-state image of Fig. 2(a) shows that annealing at 650 K produced randomly distributed chains, as in Fig. 1(a) except that dimers now appear as ovals and the dimer rows are separated by dark lines. Again, isolated adatoms and unpaired adatoms at the ends of chains were observed. Figure 2(c) summarizes the chain population as a function of the number of atoms. Tetramer and hexamer chains were the most common (~45% vs ~28%), and the average chain size was ~5 atoms. Chains of even numbers of atoms outnum-

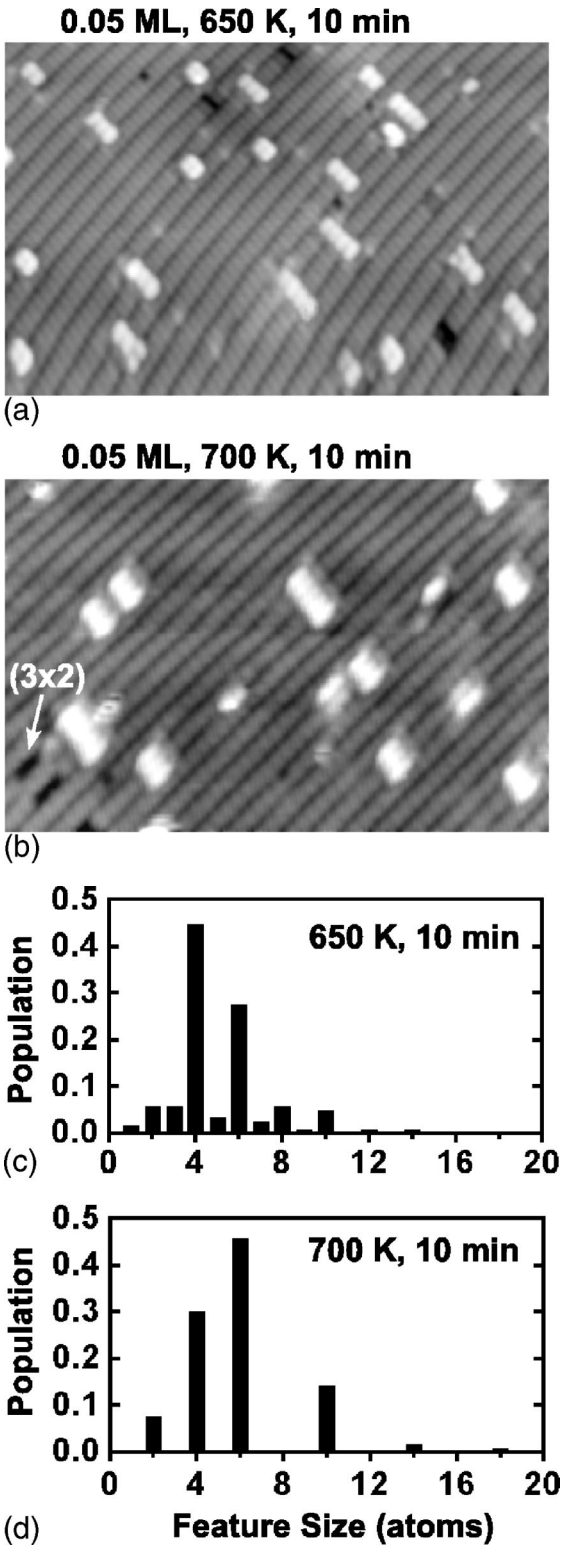

FIG. 2. (a) and (b) Representative filled-state STM images (200×130 Å^2) with 0.05 ML Si on Br-saturated Si(100) after annealing at 650 and 700 K for 10 min. The relative populations of Si chains as a function of the number of atoms in them are summarized in (c) and (d), showing conversion of odd to even chains at 700 K and chain growth. Note that the thermal drift in (a) has not been corrected, and there is slight shadow for overlayer Si chains in (b) due to the tip condition.

bered those of odd numbers by about 6 to 1. Annealing at 700 K facilitated Ostwald ripening, Fig. 2(b), as hexamers grew at the expense of tetramers (~46% vs ~30%) and chains with an odd number of atoms converted to fully dimerized chains. Analysis of this surface after annealing at 700 K indicates that the Br concentration decreased very little from Fig. 2(a), ~0.01 ML. The bottom left of Fig. 2(b) reveals small segments of (3×2) structure where two atom vacancy lines are separated by a dimer unit (each is composed of three atom vacancies as will be discussed in the next section).

C. Development of (3×2) periodicity in the Si adlayer

Sections III A and III B emphasized the low coverage regime, first for the as-deposited state and then after limited thermally activated diffusion produced more ordered structures. This section focuses on an equivalent set of results for the intermediate coverage regime. Images for the as-deposited surface with 0.3 ML Si showed a high density of bright features derived from atoms and groups of atoms that were approximately one atomic unit high.

Annealing at 600 K produced chains that were ten or more dimers in length, and most were one dimer wide. Many chains were laterally separated by one atomic unit, producing a (3×2) structure. Annealing at 650 K led to more ordering with structures that were two or three dimers wide and more evident (3×2) areas.

The separation of chains increases the distance between the Br adatoms on them and thereby reduces the Br–Br steric repulsive interactions. As discussed in detail for Br-roughened Si(100),[6] the latter are sufficiently strong that (2×1) terraces convert to (3×2) patchworks. They do so by creating atom vacancy lines. The adlayers that grew from the ejected Si also have (3×2) patches. Xu *et al.*[6] followed this roughening in real time with variable temperature STM at 700 K, and they showed that (3×2) first formed at high Br coverage but then reverted to (2×1) as the concentration diminished; (3×2) structures also form as a Si overlayer assembles in the presence of Br. In both cases, there is a reduction in total energy for (3×2) rather than (2×1) domains.

Annealing at 700 K led to improved ordering, and the enhanced surface quality made it possible to count the Br-free dimers. To our surprise, the Br coverage had decreased to ~0.8 ML. Moreover, the overlayer features had increased in size and decreased in density. While some chains were still in the 3×2 registry, others had formed (2×1) islands. This is consistent with the energetics reported by de Wijs and Selloni.[19] (3×2) was favored at saturation but was thermodynamically unstable at 2/3 ML.

The significant loss of Br probably reflects the formation of weakly bound Br atoms during Br–Si exchange. In particular, a Br atom that is coordinated with a single Si adatom would be substantially less well bound than a Br atom on an ordered Br–Si(100) terrace. Whereas the latter show very little Br loss at 700 K,[20] the former have a much greater desorption rate. This effect would be more apparent at higher Si coverage since a greater population of these unstable fea-

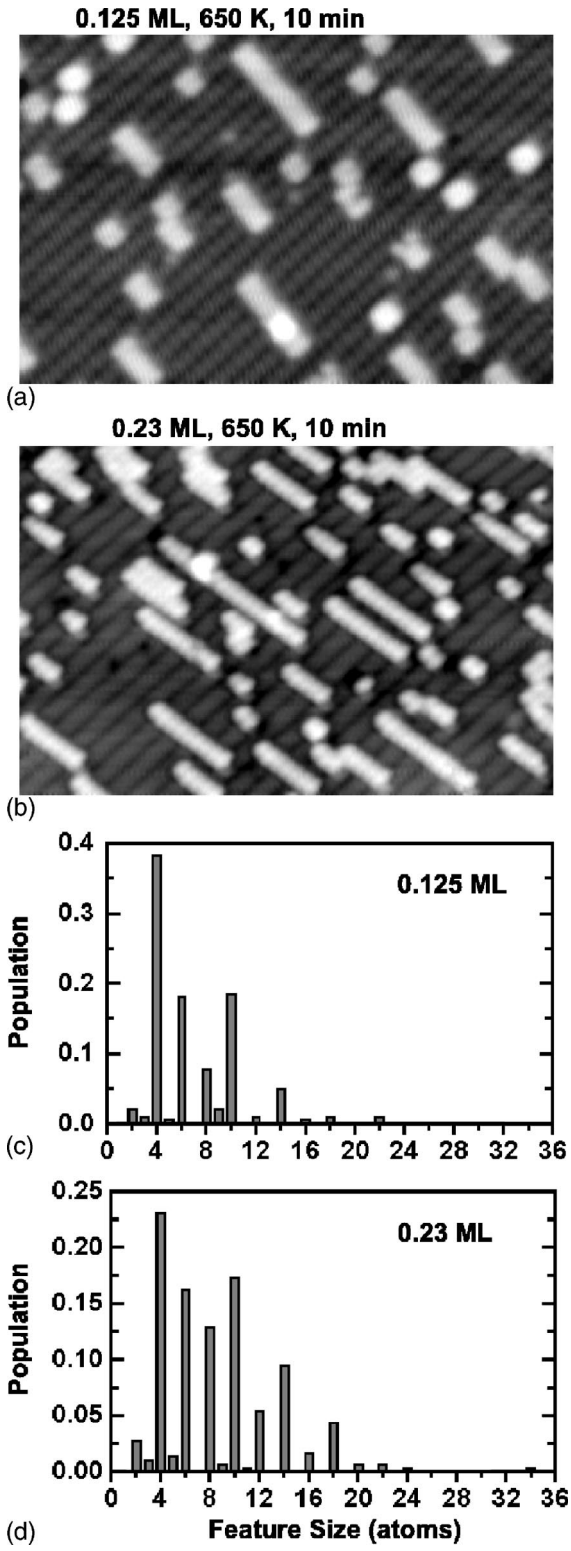

FIG. 3. (a) and (b) Filled-state images (200×130 Å^2) that show the buildup of the overlayer. The starting coverage was 0.064 ML (not shown). After each deposition, the sample was annealed for 10 min at 650 K and then imaged. Only single chains were produced at 0.125 ML, but further deposition led to the nucleation of additional chains and chain growth. The patterns were dictated by the high Br coverage and the steric repulsive interactions of those Br. The populations of chains are summarized in (c) and (d).

tures would have been formed. Indeed, the Br loss in Fig. 1(a), namely ~0.02 ML for 0.06 ML of Si adatoms, is much less than that for 0.3 ML of Si adatoms, ~0.2 ML.

D. Si coverage dependent morphologies

This section focuses on adlayer development as the amount of Si deposited increased from 0.064 to 1 ML. After each deposition, the sample was annealed at 650 K for 10 min and imaged at room temperature. Figures 3(a) and 3(b) are representative of surfaces with 0.125 and 0.23 ML of Si, respectively. The starting point in this series was 0.064 ML, and it was equivalent to that of Fig. 1(a) with an average feature size of 4.9 atoms and a feature density of 8.8 features per 100 nm^2. For 0.125 ML (0.23 ML) the chain length was 6.9 (8.5) atoms and density was 12.2 (15.3) features per 100 nm^2. The density increase points to the nucleation of new chains and hindered adatom diffusivity. Growth was limited to single layer thickness, as layer 1 formed on the substrate (layer 0).

Figures 3(c) and 3(d) give the normalized populations as a function of feature size deduced from Figs. 3(a) and 3(b). In all cases, the most common feature was a Si tetramer (two dimers). For 0.064 ML, chains ranged in size from one to ten atoms, as in Fig. 1, and the odd numbered ones represented 15.6% of the population, including ~2% that were individual adatoms. For 0.125 ML, the maximum feature size was 22 atoms, those with incomplete dimers decreased to 7.8%, and all of the individual adatoms were able to pair up or attach to a chain. At 0.23 ML, the percentage of incomplete dimer chains dropped to 3.4%. Among them, the ones with an odd number of dimers greatly outnumbered those with an even number as the end dimers of odd-dimer chains always stay in the trough, forming rebonding structures with the substrate.[21]

For coverages through 0.125 ML, only single chains were observed. This implies that any Si atoms that arrived on a chain would diffuse away at 650 K, again implicating Br–Br interactions that favored (3×2) patches over (2×1) islands. Moreover, the sticking coefficient of a dimer at an S_A step is small for the clean surface, and the presence of Br would reduce the likelihood that a dimer would be captured. At 0.23 ML, the chains started to double up, but they were almost never of the same length. This suggests that they were partnered by accident (the close proximity of their nucleation sites), that growth occurred by atom capture at the chain end, and that very little island restructuring occurred that would reduce the kink density. The latter can again be rationalized in terms of the tendency to repel individual dimers from chain sides.

Figure 4(a) shows the overlayer produced after 0.3 ML deposition. For it, the Br concentration was ~0.85 ML with most of the bare dimer sites on the chains. Indeed, about half of the dimers in the chains were Br free. Figure 4(a) also shows the onset of second layer growth, as highlighted by the circles. In the left circle, a layer-2 dimer was trapped at the junction of three layer-1 chains. Of these chains, the upper two were in-phase and the other was laterally offset by one atomic unit. The resulting junction represents an an-

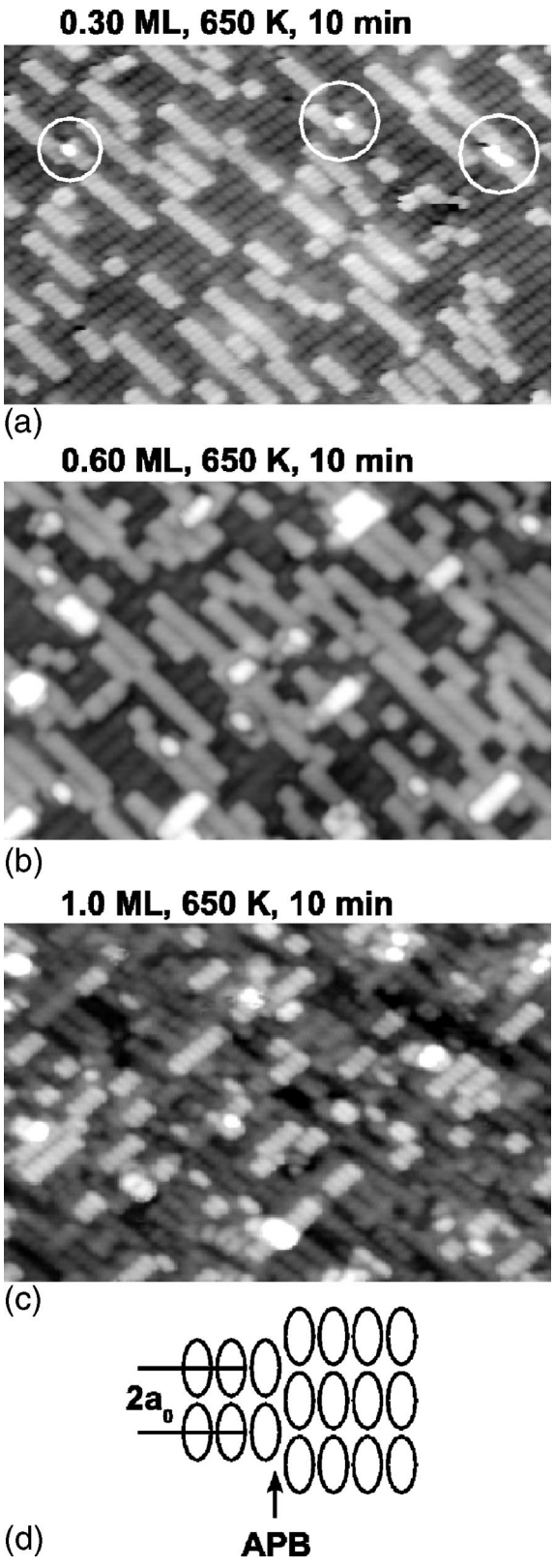

FIG. 4. (a)–-(c) reveal multilayer growth of Si on Br–Si(100). All three surfaces have followed the cycle of Si deposition at room temperature and annealing at 650 K for 10 min. Antiphase boundaries develop when chains intersect but are out of phase. These structures are preferred nucleation sites for subsequent layer chains, (d) illustrates an antiphase boundary, APB.

tiphase boundary (APB). The middle circle also shows a layer-2 dimer trapped at the APB where three layer-1 chains met. The right circle shows a two-dimer unit where only two chains at layer 1 were involved.

Figure 4(d) depicts an APB produced when chains meet, end-to-end. The experiment shows that second layer nucleation always started at this type of boundary.[22] The nucleus then grew into a chain that covered the boundary before an adjacent chain formed. Lattice strain caused by phase mismatch probably makes APBs the favored nucleation site. Note that APBs have previously been identified as nucleation sites in Si homoepitaxy, but the APB structures observed for the clean surface are different from those produced here,[23–25] and next layer nucleation occurs on islands that are much larger than those observed here.

Figure 4(b) shows that layer 1 was still highly imperfect after 0.6 ML Si deposition. As a result of the increased extent of layer 1, impinging Si adatoms could arrive on top of connected chains and further nucleation of layer 2 occurred at APBs. In some cases, layer-2 patches grew to be two dimers in width. These nascent (2×1) islands were possible because of the reduced Br concentration on the layer-1 chains. After 0.6 ML total deposition, layer 1 accounted for 0.55 ML and layer 2 accounted for the remaining 0.05 ML.

The statistics of chain phases demonstrate the importance of Br–Br steric repulsive interactions in the patterning of the top layer. If we take any chain as a reference, the phases of all other chains can be determined according to their lateral offset. For layer-1 chains, the number of in-phase and out-of-phase chains should be equal for random nucleation, regardless of the width of the growth features, i.e., whether they are small as in Fig. 4 or large as in the case of islands seen in Si homoepitaxy.[23–25] Indeed, analysis of the results for the surface of Fig. 4(b) with 553 chains in a 40×40 nm^2 area gave 277 that were in-phase and 276 that were out-of-phase. To examine the role of Br in determining local structures, we focused on each of those 553 chains and counted the number of adjacent in-phase and out-of-phase chains [the former representing chains of a (2×1) structure while the latter were (3×2)]. The results showed that the probability of finding an out-of-phase chain around any given chain was $\sim$60%. This is consistent with Br–Br steric repulsive interactions giving rise to a rough surface.

Figure 4(c) shows the morphology obtained after 0.4 ML of Si was added to Fig. 4(b) and the surface was annealed at 650 K for 10 min. Four layers are now apparent. Layer 1 is dark gray, its dimer rows run as they did in Fig. 4(a), and it is 81% complete. Vacancy lines derived from one to several dimers or from a single atomic row were frequently observed in this layer. Layer 2 accounted for 0.18 ML of Si and the chains in layer 2 were several dimers in width. Lateral expansion of Si chains was observed both in-phase and out-of-phase. The latter had a higher probability in layer 2 due to the reduced Br concentration. Layer 3 had just started to develop, as is apparent from the bright features, and it covered only 0.01 ML.

In Fig. 4(a), layer 1 covered 0.3 ML of the surface. Si adatoms deposited onto this surface would have a 30% probability of arriving on layer 1. When 0.3 ML was added, $\sim$0.09 ML would have arrived on layer 1 (30% of the 0.3 ML). Experiment showed that the extent of layer 2 was only 0.05 ML, indicating a loss of about half via diffusion from layer 1 to 0, Fig. 4(b). Similarly, further deposition of 0.4 ML onto Fig. 4(b) would yield coverages of layers 1, 2, and 3 of 0.73, 0.25, and 0.02 ML, respectively. The measured coverages were 0.81, 0.18, and 0.01 ML, respectively. Hence, $\sim$50% of the new Si adatoms diffused from layer 2 to 1 and $\sim$30% from layer 1 to 0 during the annealing cycle. Moreover, the probability of losing Si atoms from a given layer depends on the coverage of that layer since layers of the highest coverage are the most stable. Consistent with this net flux from upper to lower layers are calculations for Si diffusion on H–Si(100) that deduced effective barriers for down-diffusion across S_A and S_B steps as being lower than up-diffusion.[13]

Br termination significantly hindered the motion of Si and the effective energy barriers should be considerably larger than for clean Si.[9,26,27] The Si adatoms follow a vacancy-assisted diffusion pathway when bare sites are available after Br desorption. Since the Si adatoms do not move at room temperature, the effective diffusion barrier is at least $\sim$1.5 eV from Arrhenius considerations. Similarly, the fact that they form two-dimensional layers on the surface for 600–700 K sets the upper bound for the effective barrier, $\sim$2 eV. Using Figs. 3 and 4, we can estimate the mean displacement of Si adatoms during a 10 min annealing at 650 K to be $\sim10a_0$ where movement involved single adatoms and the jump distance was a_0. Assuming an attempt frequency of 10^{13} s^{-1} gives an effective barrier on Br-saturated Si(100) of roughly 1.8 eV. This matches the estimate from the simple Arrhenius consideration. A more accurate determination of the diffusion barrier requires a more precise temperature dependent study.

IV. CONCLUSIONS

The adsorption, diffusion, nucleation, and growth of Si on Br-saturated Si(100) have been studied with atomic scale precision. Upon arrival, Si adatoms exchange with Br but are frozen in place by Br site blocking at room temperature. Annealing to 650–700 K produces a more ordered overlayer but the density of Si overlayer features is high relative to what is observed for the clean surface and chains grow by the capture of individual Si adatoms. Increased Si deposition and annealing lead to chain coalescence. Those that intersect with others can produce antiphase boundaries that serve as nucleation sites for the next-layer growth. Detailed analyses reveal that Br–Br steric repulsive interactions play an important role in the local patterning of overlayer chains.

Comparison of the surface morphology obtained here with those in previous studies on atomic layer etching induced by Br, e.g., Fig. 8 in Ref. 18, shows a general similarity between the surface morphologies. This indicates the role of Br in determining the local patterning. In general, Br adatoms change the surface energetics of Si(100) by introducing new interactions, and they alter surface processes kinetically through site blocking.

ACKNOWLEDGMENTS

This paper was supported by the National Science Foundation and the U.S. Department of Energy, Division of

Materials Sciences under Award No. DEFG02-91ER45439, through the Frederick Seitz Materials Research Laboratory at the University of Illinois at Urbana-Champaign. Some of the experiments were performed in the Center for Microanalysis of Materials, and we acknowledge the expert assistance of V. Petrova, S. Burdin, and E. Sammann. We thank V. N. Antonov and C. M. Aldao for stimulating discussions.

[1] C. M. Aldao and J. H. Weaver, Prog. Surf. Sci. **68**, 189 (2001).
[2] K. S. Nakayama, E. Graugnard, and J. H. Weaver, Phys. Rev. Lett. **88**, 125508 (2002).
[3] C. F. Herrmann, D. Chen, and J. J. Boland, Phys. Rev. Lett. **89**, 096102 (2002).
[4] G. J. Xu, E. Graugnard, V. Petrova, K. S. Nakayama, and J. H. Weaver, Phys. Rev. B **67**, 125320 (2003).
[5] G. J. Xu, K. S. Nakayama, B. R. Trenhaile, C. M. Aldao, and J. H. Weaver, Phys. Rev. B **67**, 125321 (2003).
[6] G. J. Xu, E. Graugnard, B. R. Trenhaile, K. S. Nakayama, and J. H. Weaver, Phys. Rev. B **68**, 075301 (2003).
[7] C. M. Aldao, S. E. Guidoni, G. J. Xu, K. S. Nakayama, and J. H. Weaver, Surf. Sci. **551**, 143 (2004).
[8] Y.-W. Mo, B. S. Swartzentruber, R. Kariotis, M. B. Webb, and M. G. Lagally, Phys. Rev. Lett. **63**, 2393 (1989).
[9] G. Brocks, P. J. Kelly, and R. Car, Phys. Rev. Lett. **66**, 1729 (1991).
[10] M. Copel and R. Tromp, Phys. Rev. Lett. **72**, 1236 (1994).
[11] J. Nara, T. Sasaki, and T. Ohno, Phys. Rev. Lett. **79**, 4421 (1997).
[12] S. Jeong and A. Oshiyama, Phys. Rev. Lett. **79**, 4425 (1997).
[13] S. Jeong and A. Oshiyama, Phys. Rev. Lett. **81**, 5366 (1998).
[14] S.-J. Kahng, Y. H. Ha, J.-Y. Park, S. Kim, D. W. Moon, and Y. Kuk, Phys. Rev. Lett. **80**, 4931 (1998).
[15] S.-J. Kahng, J.-Y. Park, and Y. Kuk, Phys. Rev. B **60**, 16 558 (1999).
[16] Wolkow (Ref. 17) observed Si adatom pairing on Si(100) at 160 K where the paired atoms were coupled through a substrate-mediated interaction but not a direct chemical bond.
[17] R. A. Wolkow, Phys. Rev. Lett. **74**, 4448 (1995).
[18] K. Nakayama, C. M. Aldao, and J. H. Weaver, Phys. Rev. B **59**, 15 893 (1999).
[19] G. A. de Wijs and A. Selloni, Phys. Rev. B **64**, 041402(R) (2001).
[20] B. R. Trenhaile, V. N. Antonov, G. J. Xu, K. S. Nakayama, and J. H. Weaver, Phys. Rev. Lett. (to be published).
[21] D. J. Chadi, Phys. Rev. Lett. **59**, 1691 (1987).
[22] The other type of out-of-phase boundary is the (3×2) structure.
[23] R. J. Hamers, U. K. Kohler, and J. E. Demuth, Ultramicroscopy **31**, 10 (1989).
[24] P. Bedrossian and E. Kaxiras, Phys. Rev. Lett. **70**, 2589 (1993).
[25] M. J. Bronikowski, Y. Wang, and R. J. Hamers, Phys. Rev. B **48**, 12 361 (1993).
[26] Y.-W. Mo, J. Kleiner, M. B. Webb, and M. G. Lagally, Phys. Rev. Lett. **66**, 1998 (1991).
[27] J. L. Iguain, H. O. Martin, C. M. Aldao, Y. Gong, S. J. Chey, and J. H. Weaver, J. Vac. Sci. Technol. A **16**, 3460 (1998).